

2D Janus Hybrid Materials of Polymer-Grafted Carbon Nanotube/Graphene Oxide Thin Film as Flexible, Miniature Electric Carpet

Peng Xiao, Changjin Wan, Jincui Gu, Zhenzhong Liu, Yonghong Men, Youju Huang,* Jiawei Zhang,* Liqiang Zhu, and Tao Chen*

Ultrathin, freestanding polymer hybrid film with macroscopic sizes and molecular thicknesses have received significant interest due to their applications as functional devices, microsensors or nanoactuators. Herein, a 2D Janus hybrid of polymer-grafted carbon nanotubes/graphene oxide (CNTs/GO) thin film is fabricated using microcontact printed CNTs/GO as photo active surface to grow polymer brushes by self-initiated photografting and photopolymerization selectively from one side of CNTs/GO film. This achieved 2D Janus hybrid materials with grafted polymer layer as insulative carpet and supported CNTs/GO thin film as conductive element have the potential application as flexible and miniature electric carpet for heating micro-/nano devices locally.

development by Sharp and co-workers^[3] to construct polymer brushes-grafted single layer graphene allows the polymer carpet with high conductivity. We have also developed a surface modification strategy to achieve functional polymer carpet with low conductivity through microcontact printing (μ CP)-induced supramolecular self-assembly of graphene oxide (GO) as the supported substrate to grow polymer brushes from photoactive site of HO-groups on GO by self-initiated photografting and photopolymerization (SIPGP).^[4a,b]

Named after the two-faced Roman God Janus, the concept of Janus particles comprising multiple compositions and functionalities was introduced by P. G. de Gennes in 1991.^[5] The term of Janus has thus been extended to describe materials having different properties at opposite sides.^[6] Chemistry in 2D differs significantly from chemistry in 3D, which resulted in the recent interest in thin free-standing 2D Janus materials, such as nanosheets or nanomembranes.^[7a,b] These nanomaterials even could be transported from one environment to another one without losing their structural integrity, providing new opportunities for 2D chemistry. Sharp and our strategies stated above have shown the successful fabrication of polymer-grafted graphene or GO as Janus thin film structure, which endows the graphene or GO thin layer with polymer chemical functionality, and gives the polymer with grapheme-based properties. However, due to the significantly high conductivity of graphene and significantly low conductivity of GO,^[8a,b] such freestanding 2D thin film can hardly be integrated as the miniature electric carpet.

Carbon nanotubes (CNTs), invented by Iijima and Ichihashi in the early 1990s,^[9] have obtained continuous interest due to their unique physical, chemical, and electrical properties,^[10a-f] which render them attractive candidates in versatile prospective potential applications in supercapacitors,^[11a,b] transistors,^[12a-e] pressure sensors,^[13a-c] and electrical wiring.^[14] By employing a series of strategies, such as wetting spinning,^[15a,b] chemical vapor deposition synthesis,^[16] and even achieving CNTs yarns from super-aligned arrays,^[17] a standard conductive wire,^[18] or Ethernet cable,^[14] etc. have already been achieved. These current endeavors largely rely on the adjustable conductivity/semi-conductivity of the CNTs,^[19a,b] which inspire us to introducing CNTs into the 2D Janus hybrid thin film as conductive element inside polymer carpet.^[20]

1. Introduction

As a contacting type electric heating appliance, electric blanket or carpet plays a significant role in keeping warm in large parts of South China, where there is no heating system yet very cold and wet in winter. Using these electric carpets, people can also reduce the pain of rheumatism besides keeping warm. By the enlightenment of effectively being relieved of rheumatism pain, it was even developed into miniaturization as joint therapeutic apparatus and used in any time upon occurrence of the pain of rheumatism. Inspired by the electric carpet, there was a recent report about polymer carpet by Jordan and co-workers,^[1a,b] who named a freestanding polymer brush fabricated by surface-initiated polymerization from a cross-linked 1 nm-thick monolayer as polymer carpet. The solid-supported polymer carpets are found to be mechanically robust and to react instantaneously and reversibly to external stimuli by buckling, which have the potentials in the development of completely new integrated micro-/nanotechnology devices.^[2a-d] Their creative work allows exploring the potential of polymer carpet as the miniature electric carpet through the introduction of appropriately conductive element beneath the polymer layers. Further

P. Xiao, C. Wan, J. Gu, Z. Liu, Y. Men, Dr. Y. Huang, Dr. J. Zhang, Dr. L. Zhu, Prof. T. Chen
Ningbo Institute of Material Technology and Engineering
Chinese Academy of Science
Ningbo 315201, China
E-mail: yjhuang@nimte.ac.cn; zhangjiawei@nimte.ac.cn;
tao.chen@nimte.ac.cn



DOI: 10.1002/adfm.201404624

Herein, we present our recent advancement in fabricating polymer brushes-grafted CNTs as 2D Janus hybrid thin film, which could be used as a flexible and miniature electric carpet in the combination of grafted polymer layer as insulative carpet and supported carbon materials as conductive element. To prove this concept, μ CP was used to construct the micropatterned CNTs which work like the resistance wire inside real electrical carpet. Although μ CP has been used to induce the supramolecular self-assembly from small molecules to micro-sized GO nanosheets onto OH-terminated silicon substrates via hydrogen bonds,^[4] it is very difficult for CNTs as the ink during the μ CP process because CNTs cannot form a homogenous and stable dispersion in solvents. Since GO has been viewed previously as an amphiphile with hydrophobic basal plane and hydrophilic edges, it might disperse CNTs effectively based on the π - π interaction.^[8a,21a,b] The hybrid ink of CNTs/GO with an adjustable conductivity was thus used during μ CP process at the first time to construct microstructured carbon-based thin film.^[8a] Photoactive HO-groups on CNTs or GO could be initiated to grow polymer brushes by SIPGP from CNTs/GO thin film, which allows the fabrication the 2D Janus hybrid thin film in a simple strategy. The obtained polymer carpet-grafted CNTs/GO thin films has the potential application as flexible, transparent, and miniature electric carpet for warming micro-/nano devices locally.

2. Results and Discussion

Our strategy for fabricating polymer brushes-grafted CNTs/GO as 2D Janus hybrid thin film and subsequent etching as a freestanding flexible miniature electric carpet is schematically illustrated in **Figure 1**. GO functionalized CNTs in ethanol solution could be used to ink polydimethylsiloxane (PDMS) stamp, which was firstly contacted with fresh piranha solution-treated

silicon substrate (**Figure 1A**). Force-induced effect provided multiple hydrogen bonds between CNTs/GO and hydroxylated silicon surface.^[4] Based on the differing interaction strengths of PDMS-CNTs/GO and CNTs/GO-substrate interfaces, CNTs/GO was transferred from PDMS stamp onto silicon wafer during μ CP (**Figure 1B**).^[22a-c] Photoactive groups existing on CNTs and GO offered alternative active sites for grafting polymers by SIPGP (**Figure 1C**). This polymer brushes-grafted CNTs/GO as 2D Janus hybrid thin film can be further lifted off from the silicon substrate using alkaline media as etching agent (**Figure 1D,E**). The as-prepared freestanding 2D Janus hybrid thin film could be transferred onto any substrate for further particular applications (**Figure 1F**).

Since CNTs could not be used as the ink directly during μ CP due to the difficulty in forming a homogenous and stable dispersion in solvents (**Figure S1A**, Supporting Information), GO (**Figure S1B**, Supporting Information) with perfect dispersion in ethanol was used to functionalize and induce the dispersion of CNTs owing to strong π - π stacking interactions. For fabricating CNTs/GO with different ratios, it is necessary to employ appropriate surfactant to form stable dispersion.^[23a,b] Whereas, using an adequate ratio of CNTs/GO,^[8a] CNTs with the diameter ranging from 15 to 25 nm (**Figure 2A**) and GO with thickness ≈ 1.3 nm and nanosheets size in the range of ≈ 0.5 – 2 μ m (**Figure 2B**) can form a homogenous solution in ethanol (**Figure S1C**, Supporting Information), which could be used as ink directly during μ CP. Based on the hydrogen bonds between ink and substrate, well-defined architectures can be ascertained with thickness about 35 nm (**Figure 2C**), which suggested two layer CNTs thin film interacted with hydroxylated silicon surface was achieved. Further observation about CNTs and GO sheets could be seen clearly from the magnification atomic force microscopy (AFM) image in **Figure 2D**, in which CNTs has a fine dispersion in consistent with the state of CNTs in solution. As displayed by our previous work, the photoactive sites

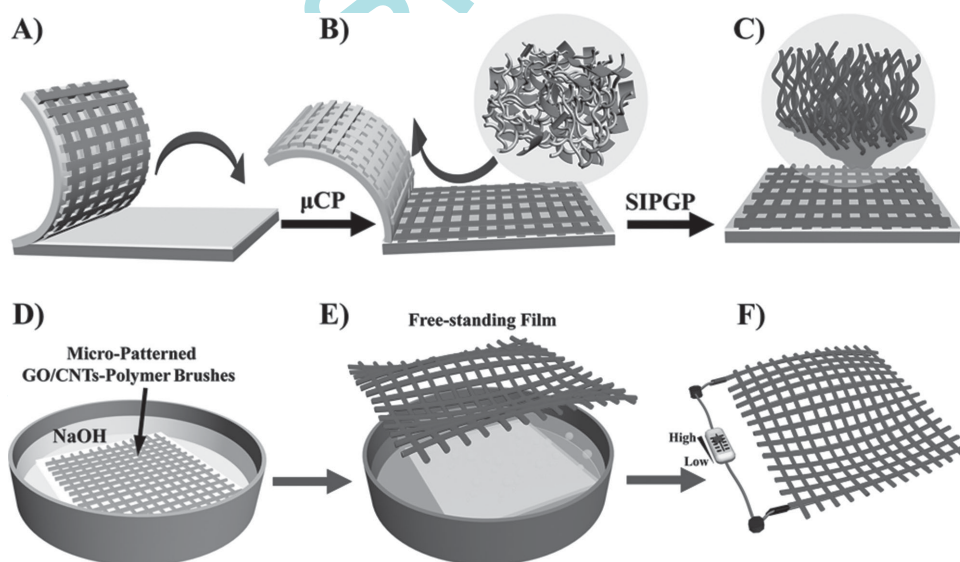


Figure 1. Schematic procedure of fabricating 2D Janus hybrid materials of polymer-grafted CNTs/GO thin film via μ CP-induced CNTs/GO assembly, subsequent SIPGP, and final etching process. A) Inking of PDMS stamp. B) Selective transfer and patterning of CNTs/GO by μ CP. C) Subsequent pattern amplification by SIPGP. D) Immersing patterned polymer brushes in NaOH solution. E,F) After etching, a transparent film floating and could be transferred to any substrate or assembly as a device.

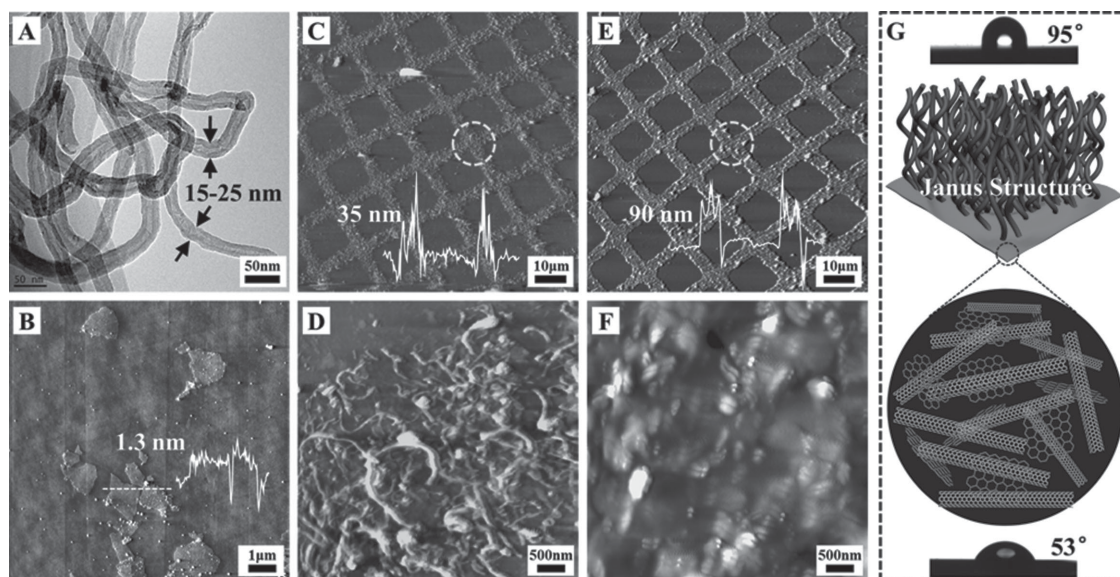


Figure 2. A) TEM images of CNTs. Tapping mode of AFM height images imaged at room temperature in air: B) GO sheets ($10\ \mu\text{m} \times 10\ \mu\text{m}$); C) Bare patterned CNTs/GO ($90\ \mu\text{m} \times 90\ \mu\text{m}$); D) the enlarged image of CNTs/GO ($5\ \mu\text{m} \times 5\ \mu\text{m}$); E) PS-grafted CNTs/GO on silicon surface by SIPGP ($90\ \mu\text{m} \times 90\ \mu\text{m}$); F) The enlarged image of PS-grafted CNTs/GO ($5\ \mu\text{m} \times 5\ \mu\text{m}$). G) Schematic plot of the Janus structure in composition of CNTs/GO-based PS and in wettability of WCA.

on CNTs and GO surface make it significantly simple to grow various vinyl polymers from carbon-based materials.^[4a,24a,b] This technique provides possibility for the fabrication of 2D Janus hybrids carbon thin film with polymer layer directionally coating on one side of the carbon thin film and leaving another side of the carbon thin film free. After the polymerized magnification by SIPGP, AFM image in Figure 2E further shows the resulting patterned polymer carpet with a thickness about 90 nm, whose sizes and shapes are in good agreement with those of CNTs/GO. From the amplified image, we can clearly observe that CNTs and GO are fully grafted with polymers (Figure 2F). This achieved hybrid thin film has respective advantage of polymer layer in insulation and CNTs/GO film in adjustable conductivity. Water contact angle (WCA) measurement was also used to investigate the surface wettability properties before and after the UV-irradiation reaction during the grafting of polymer brushes on micropatterned CNTs/GO thin film. Before SIPGP through UV-irradiation, the WCA of CNTs/GO films was about 53° (Figure 2G), which is consistent with the abundant hydroxyl and carboxyl functional groups on CNTs/GO. Once styrene was mixed with the CNTs/GO film, polystyrene (PS) brushes were grafted on the CNTs/GO film upon the UV irradiation (intensity maximum at $\lambda = 365\ \text{nm}$ with power about $240\ \text{mW cm}^{-2}$), and displays a WCA value of 95° (Figure 2G). The more hydrophobic properties of PS-grafted CNTs/GO films indirectly evidenced the successful grafting of PS, and showed a Janus structure also in wettability difference of each side. It should be noted that although PS brushes were grafted on CNTs/GO films as the proof-of-concept, various monomers could also be employed during SIPGP to functionalize the CNTs/GO film. The hydrophilic poly (*N,N*-dimethylaminoethylmethacrylate) (PDMAEMA) brushes-grafted CNTs/GO film show a WCA value of 28° (Figure S2A, Supporting Information). More interestingly, the pore size of microstructured CNTs/GO thin film

could be adjusted by applying different force on stamp during $\mu\text{CP}^{[25]}$ (Figure S3, Supporting Information). The generic nature of SIPGP could most likely be used to be extended for designing different polymer brushes in chemical composition and various thickness of the polymer layer by varying the polymerization time (Figure S4, Supporting Information).^[1a,4a]

The freestanding 2D Janus hybrid materials of polymer-grafted CNTs/GO thin film with the transparent and hydrophobic properties, could be achieved using alkaline media as etching agent and then be transferred to any substrates (Figure 3A). Notably, after several times rinsing in water, the mechanical strength of the polymer-grafted CNTs/GO composite is still robust enough to support itself floating on the water surface without any fracture. Additionally, as previously reported by Li and co-workers,^[26] chitosan (CS)-grafted reduced GO (rGO) dispersed multiwalled CNTs (MWCNTs) film has demonstrated strengthened mechanical properties, such as modulus, strength, and so forth, compared with GO, MWCNTs and CS-rGO. Thus, it is predicted that in the polymer-grafted CNTs/GO hybrids system, the hybrids may be much more prominent. However, more detailed mechanical properties will be further explored by employing precisely controlled method for potential applications in actuators.^[1a] In order to investigate the electric information of the 2D Janus hybrid thin film, patterned Al electrodes were chosen as the target substrate. The optical image in Figure 3B further demonstrates the transferred 2D Janus hybrid thin film with a well-controlled height and a feature space at $10\ \mu\text{m}$ in a large area. More morphology information was confirmed further by AFM (Figure 3C), indicating the resulting 2D Janus hybrid thin film with an average thickness about 83 nm, which is consistent with the AFM image before etching. The resulted 2D hybrid thin film is larger than 1 cm in lateral dimensions with thickness about 80–90 nm, demonstrating a stable structure floating on the water.

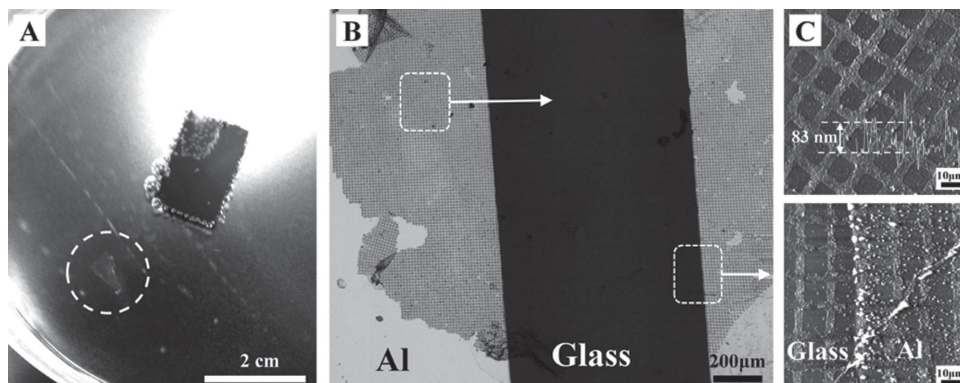


Figure 3. A) Photograph of freestanding miniature electric carpet floating on the alkaline solution surface, which is released from silicon substrate. B) Optical image of miniature electric carpet transferring onto Al electrodes surface in reflection mode. C) AFM images of miniature electric carpet on different locations of electrodes surface.

Nevertheless, larger ultrathin film results in more wrinkles for stabilizing the 2D structure. It is noted that after etching also, there may be some ruptures occurring in the film with large dimensions, due to some inevitable defects induced by wrinkles whereas, for the successful fabrication of large-area micro-devices, the 2D free-standing film needs further improvement. Additionally, SEM was also employed to explore the surface morphology of the free-standing thin film, demonstrating a patterned structure fully covered with polymer brushes (Figure S5, Supporting Information). Actually, as marked by red arrows, some wrinkles of CNTs/GO hybrids were clearly observed. Furthermore, in order to acquire more detailed morphology information of the integral film, TEM images were obtained

by transferring the free-standing thin film onto the copper grid surface (Figure S6A, Supporting Information). As shown in Figure S6B–D (Supporting Information), both CNTs and GO were densely grafted by polymer brushes for improving stabilization and insulation properties.

A different optical microscope mode was used to observe the full information of the freestanding film due to the remarkable difference of transparency between Al electrodes and glass substrate (Figure 4A inset). As shown by reflection and transmission mode measured in the same area (Figure 4A,B), the hybrid thin film presents a flexible and intact structure, which spreads on the substrate and effectively bridges the isolated electrodes. The resulting freestanding 2D Janus hybrid thin film not only

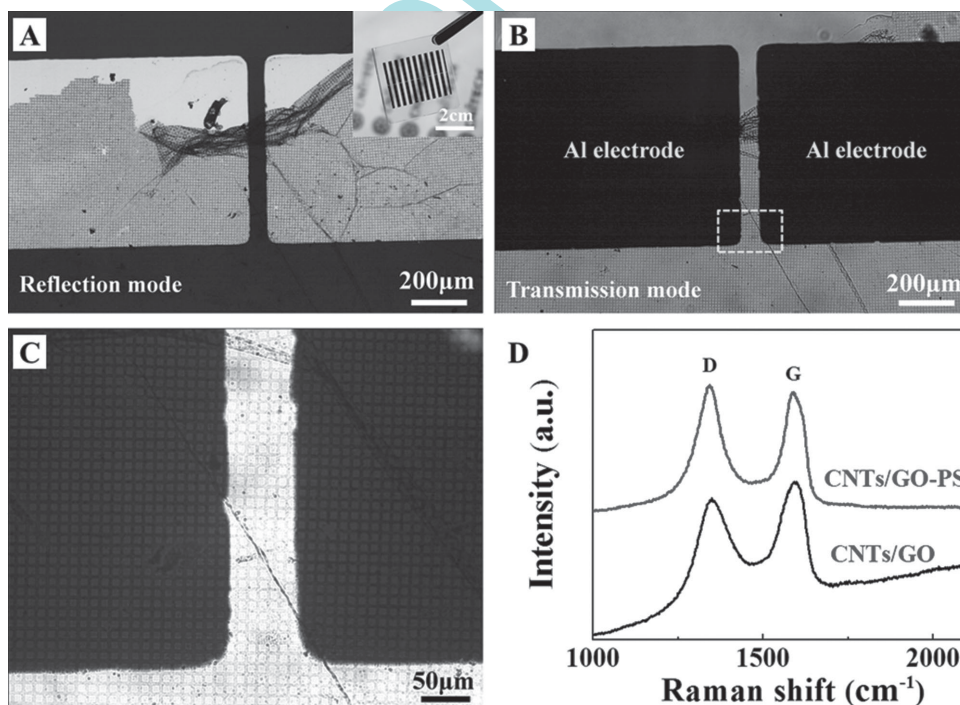


Figure 4. Optical images of freestanding 2D Janus hybrid materials of polymer-grafted CNTs/GO thin film transferred onto parallel Al electrodes surface. Reflection and transmission mode of optical microscope are employed in (A,B). C) Corresponding magnified image of (B) in transmission mode. D) Raman spectra of CNTs/GO and CNTs/GO-PS.

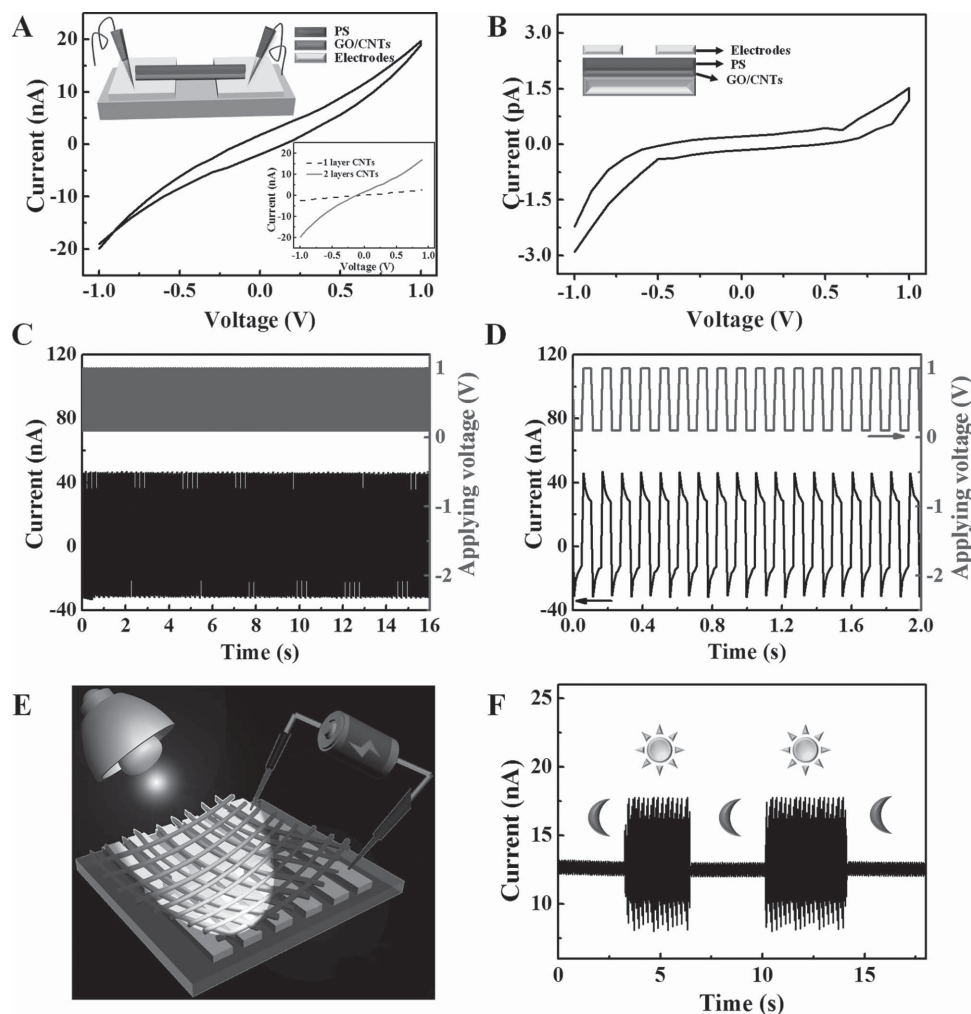


Figure 5. A) Current–voltage curves of the freestanding 2D Janus hybrid materials of polymer-grafted CNTs/GO thin film. Inset, current–voltage curves of the freestanding 2D Janus hybrid thin film with different CNTs/GO layers. B) Current–voltage curve of the parallel electrodes deposited on CNTs/GO-based PS surface. C) $I-t$ and $V-t$ curves of transient response, at 100 ms for each cycle. D) The detailed curves of transient response. E) Schematic diagram of 2D Janus hybrid materials of polymer-grafted CNTs/GO thin-film circuit irradiated by light. F) Current versus time in the absence and presence of light.

has well-defined structures, but also shows robust, continuous macroscopic and defect-free structures. Figure 4C with a magnified area further demonstrates the transferred 2D Janus hybrid thin film with a well-controlled height and a feature space at 10 μm in a large area.

For acquiring more information on the development of CNTs/GO films during the UV irradiation process with or without monomers, Raman spectra of CNTs/GO, CNTs/GO-PS, and CNTs/GO-PDMAEMA were obtained to explore the reduction and grafting behavior via SIPGP. As shown in Figures 4D and S2B, (Supporting Information) CNTs/GO shows the significant characteristic spectrum of the D and G mode with I_D/I_G of 0.90. However, following SIPGP, Raman spectra of PS and PDMAEMA-grafted CNTs/GO films display the larger ratio of I_D/I_G about 1.06 and 1.15, respectively. Compared with CNTs/GO, the larger I_D/I_G resulted from the contribution of the PS and PDMAEMA alternatively grafted from CNTs/GO and potential flash reduction of GO during SIPGP.^[4a]

In order to take the freestanding 2D Janus hybrid thin film as a polymeric electrical carpet for heating locally, several important parameters, such as the conductivities, dielectric properties, and electrical stabilities should be considered. We have integrated 2D Janus hybrid materials of PS-grafted CNTs/GO films as two-terminal devices. Inset in Figure 5A illustrates the sample structure of two patterned Al films with a distance of about 60 μm used as the electrodes. $I-V$ curve is obtained by using a semiconductor parameter analyzer. As shown in Figure 5A, the 2D Janus hybrid thin film including 35-nm thickness of about two layer CNTs exhibited nonlinear, symmetric $I-V$ characteristics, indicating a Schottky barrier existed at the CNTs/Al interface.^[27] The maximum absolute current of ≈ 20 nA was obtained at the bias of -1.0 and 1.0 V. The dash line in Figure 5A is an $I-V$ curve for the freestanding 2D Janus hybrid thin film including 20-nm thickness of about one layer CNTs. Again, a nonlinear, symmetric $I-V$ characteristic is exhibited. However, the maximum absolute current is only ≈ 2 nA. Such

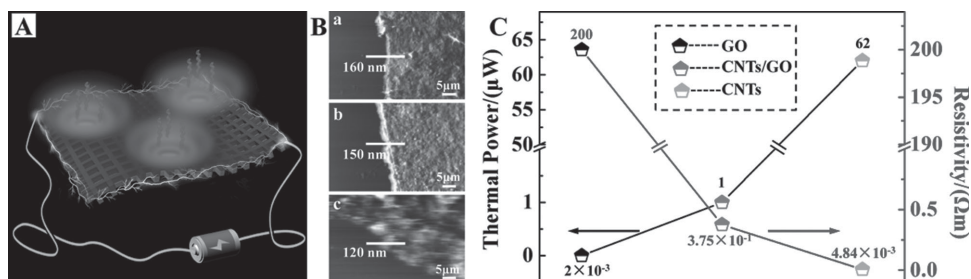


Figure 6. A) Schematic diagram of flexible and miniature polymer electric carpet. B) AFM morphology images of carbon-based films: a) GO; b) CNTs/GO; c) CNTs. C) Thermal power (black line) and resistivity (blue line) properties of GO sheets, CNTs/GO composites and CNTs after 30 min reduction by UV light.

results indicate that high conductance can be achieved by further increasing the thickness of CNTs/GO film. Whereas three or more layers of CNTs/GO will result in an unstable state of CNTs/GO self-assembled layers. They will be easy to lift off from substrate surface during SIPGP, washing steps, etching, and transferring process. Therefore, appropriate thickness of layers plays an important role in fabricating robust freestanding 2D Janus hybrid thin film.

The dielectric property of the polymer layer inside the 2D Janus hybrid materials should also be taken into consideration. We have deposited patterned IZO films on polymer layer as the electrodes (Figure S7, Supporting Information). Thanks to the fully covered polymer layer, the 2D Janus hybrid thin films present both excellent mechanical and antielectric leakage behaviors. Figure 5B shows the I - V curve of patterned CNTs/GO-PS thin film (about two layer CNTs and polymer brushes with 50-nm thickness). A maximum absolute current is only ≈ 3.0 pA, demonstrating a high resistance for polymer layer inside the 2D Janus hybrid materials. Furthermore, the thickness of insulated layers could be controlled by varying the polymerization time during SIPGP (Figure S4, Supporting Information). Notably, such a device structure can ensure safety and efficiency, when the electronic device works under some specific fields. Moreover, it is worth noting that the stability of polymer electric carpet is of great importance. Transient response of polymer electric carpet to a square-shaped pulse with width of 100 ms and amplitude of 1.0 V is shown in Figure 5C. The device exhibits a good reproducibility. No current loss is observed during 160 cycles, indicating a very good electrical stability. Figure 5D shows the detailed current curve of the transient response, in which the current can reach as high as 45 nA at the initial of the 1.0 V pulse.

Carbon-based materials always show a very good ability in photoelectric effect. Photoresponsive experiments for the freestanding 2D Janus hybrid thin film were also performed (Figure 5E). While the thickness of the polymer electric carpet is ≈ 83 nm, it is transparent enough to be penetrated by visible light into inner CNTs/GO layers. Figure 5F shows the time response of photoconductive polymer electric carpet to a bulb light.^[28] A slight vibrate with mean current value of ≈ 11.8 nA and standard deviation (σ_{off}) of ≈ 0.6 nA were observed with the light off. A violent fluctuation with mean current value of ≈ 12.2 nA and standard deviation (σ_{on}) of ≈ 5.2 nA were observed with light on. The current fluctuation with light off could be resulted from the ambient noise while the current fluctuation

with light on could be resulted from the carrier movement in the CNTs. Such results indicate the freestanding 2D Janus hybrid thin film has the potential to function as solar-energy-charged polymer electric carpet.

Since the basic parameter of the miniature polymeric electric carpet (the miniature model displayed in Figure 6A) is in consistence with a real electrical carpet, we used homogenous films of GO, CNTs/GO, and CNTs to demonstrate the CNTs/GO may exhibit prominent thermal power improvement. To validate our hypothesis, three kinds of homogenous films of GO, CNTs/GO, and CNTs were transferred on electrodes surfaces, followed by UV reduction for appropriate time to achieve appropriate reduction of GO (Figure 6B).^[8b] As shown in Figure 6C (blue line), the line resistivity of GO, CNTs/GO, and CNTs are 200, 3.75×10^{-1} and 4.84×10^{-3} Ω m, respectively. The thermal powers (P) of three films were also estimated by the formula, $P = I^2R$. In our measurement, $R = R_C + \rho l$, where R_C is the contact resistance, ρ is the line resistivity, and l is the line length between two electrodes. Here, R_C can be negligible, thus the thermal power are estimated to 2×10^{-3} , 1 and 62 μW for GO, CNTs/GO, and CNTs, respectively (black line in Figure 6C). Therefore, for achieving both a tailored morphology and relatively appropriate conductivity, CNTs/GO (2/1 wt%) ink is regarded as the optimal alternative to construct the core layer of polymer electric carpet.^[13] For this, polymer electric carpet circuit of two layers CNTs, we have demonstrated that the thermal power is approximately 0.02 μW , allowing potential applications in heating micro-/nanodevices locally. Furthermore, the conductivity and corresponding heating power can be effectively adjusted by further UV reduction of GO.

3. Conclusion

In summary, we have demonstrated a significant advancement in polymer carpet by grafting polymer from micropatterned CNTs/GO thin film as 2D Janus hybrid materials, which could be applied as a flexible and miniature electric carpet by integrating grafted polymer layer as insulative carpet and supported carbon materials as conductive element. GO functionalized CNTs could be used as hybrid ink of CNTs/GO with adjustable conductivity during microcontact printing to construct firstly microstructured carbon-based thin film based on multiple hydrogen bonds. Photoactive sites on CNTs/GO allow the subsequent growth of polymer brushes by SIPGP to achieve a

2D Janus hybrid thin film. Followed by an etching process, the freestanding miniature polymeric electric carpet can be easily transferred onto any substrate, which indicated appropriate conductivity of CNTs/GO thin film, high insulativity of polymer layer. This 2D hybrid thin film also showed the photoconductivity upon the trigger by the irradiation of a bulb. This resulted polymer carpet-grafted CNTs/GO thin films have the potential application as flexible and miniature electric carpet for heating micro-/nano devices locally. This hybrid material system could be used to enhance the promising potentials of carbon-based materials in the application of electronic filed by the nature of stimuli-responsive polymer materials for detection.

4. Experimental Section

Materials: General chemicals in chemical reagent grade were used as received from Sinopharm Chemical Reagent. Toluene, ethyl acetate, ethanol, and deionized water were used as rinsing solvents. Styrene (99%) was obtained from Alfa Aesar China (Tianjin) Co., Ltd, which was purified by neutral Al₂O₃ column and dried with a 0.4-nm molecular sieve at room temperature for 3 d. PDMS stamps with strip and grid structures were fabricated from Sylgard 184 (the ratio between component A and B was 1:10) on a silicon master. Silicon wafers and glasses were cleaned in a mixture of H₂O₂/H₂SO₄ (1:3, v/v) at 80 °C ("piranha solution") for 2 h and washed thoroughly with Milli-Q-grade water. (Caution: Piranha solution reacts violently with organic matter!).

Preparation of Homogenous Dispersion of Carbon Nanotubes/Graphene Oxide (CNTs/GO) Aqueous Solution: Graphene oxide (GO) sheets were synthesized by a modified Hummers' method and exfoliation of graphite oxide was achieved by a strong ultrasonication method. The obtained brown dispersion was then washed and centrifuged to remove any unexfoliated graphite oxide. The diameter of final GO sheets was less than 2 μm. Carbon nanotubes were obtained from Chengdu Organic Chemicals Co., LTD, Chinese Academy of Sciences, which was used as received. Grapheme oxide powders were suspended in ethanol by sonication for 4 h, giving a homogenous dispersion of GO. Then some CNTs were added into the GO solution with sonication for several hours. Finally, a homogenous suspension of CNTs/GO composites with weight ratios of 2/1 was formed for subsequent patterning.

Microcontact Printing: The PDMS stamp was inked by exposing the stamp features to an ethanol solution of CNTs/GO for 3 min and drying with nitrogen, before being brought into contact with substrates surface for 1 min to fabricate the patterned SAMs on silicon.

Self-initiated Photografting and Photopolymerization (SIPGP): The patterned polymer brushes were synthesized following a procedure introduced by Amin et al.^[1] The patterned substrate surface was submerged in ≈2 mL of distilled and degassed bulk monomer and irradiated with an UV fluorescent lamp with a spectral distribution between 300 and 400 nm distribution (intensity maximum at λ = 365 nm with a total power of ≈240 mW cm⁻²) for required time (PS for 1 h, PDMAEMA for 50 min). Following SIPGP, the functionalized films were exhaustively rinsed with different solvents (toluene, ethyl acetate, and ethanol for styrene) following ultrasonication for several minutes in order to remove any physisorbed polymer.

Fabrication of Freestanding Patterned Films: Freestanding patterned films were fabricated by transferring from the silicon substrate onto patterned electrode surface. For that purpose, the patterned polymer brushes were cleaved from the silicon surface by immersing the silicon wafer in NaOH solution (1 M) overnight.

Characterization: Atomic force microscopy (AFM) images were taken by a multimode AFM (Being Nano-Instruments, Ltd) operating in the contact and/or tapping mode using silicon cantilevers (spring constant: 0.15 N m⁻¹, resonant frequency: 12 KHz for cantilever of contact mode, spring constant: 3–40 N m⁻¹, resonant frequency: 75–300 KHz

for cantilever of tapping mode). Static WCAs were measured at room temperature using the sessile drop method and image analysis of the drop profile. The instrument (OCA-20, Dataphysics) used a charge-coupled device (CCD) camera and an image analysis processor. The water (Milli-Q) droplet volume was 3 μL, and the contact angle was measured after the drop was stable on the sample. For each sample, the reported value is the average of the results obtained on three droplets. The Raman scattering measurements were performed at room temperature on a Raman system (inVia-reflex, Renishaw) with confocal microscopy. The solid-state diode laser (532 nm) was used as an excitation source with a frequency range of 3200–1000 cm⁻¹. Electrical measurements of devices were performed with a semiconductor parameter analyzer (Keithley 4200).

Supporting Information

Supporting Information is available from the Wiley Online Library or from the author.

Acknowledgements

We thank the Chinese Academy of Science for Hundred Talents Program, Chinese Central Government for Thousand Young Talents Program, Natural Science Foundation of China (Grant Nos. 51303195 and 21304105), Ningbo Science and Technology Bureau (Grant No. 2014B82010), and Excellent Youth Foundation of Zhejiang Province of China (Grant No. LR14B040001).

Received: December 31, 2014

Revised: January 31, 2015

Published online: February 27, 2015

- [1] a) I. Amin, M. Steenackers, N. Zhang, A. Beyer, X. H. Zhang, T. Pirzer, T. Hugel, R. Jordan, A. Golzhauser, *Small* **2010**, *6*, 1623; b) I. Amin, M. Steenackers, N. Zhang, R. Schubel, A. Beyer, A. Golzhauser, R. Jordan, *Small* **2011**, *7*, 683.
- [2] a) F. Zhou, W. T. S. Huck, *Chem. Commun.* **2005**, 5999; b) K. Fries, S. Samanta, S. Orski, J. Locklin, *Chem. Commun.* **2008**, 6288; c) T. L. Sun, G. J. Wang, L. Feng, B. Q. Liu, Y. M. Ma, L. Jiang, D. B. Zhu, *Angew. Chem. Int. Ed.* **2004**, *43*, 357; d) T. Chen, R. Ferris, J. M. Zhang, R. Ducker, S. Zauscher, *Prog. Polym. Sci.* **2010**, *35*, 94.
- [3] M. Steenackers, A. M. Giegler, N. Zhang, F. Deubel, M. Seifert, L. H. Hess, C. H. Y. X. Lim, K. P. Loh, J. A. Garrido, R. Jordan, M. Stutzmann, I. D. Sharp, *J. Am. Chem. Soc.* **2011**, *133*, 10490.
- [4] a) P. Xiao, J. Gu, J. Chen, J. Zhang, R. Xing, Y. Han, J. Fu, W. Wang, T. Chen, *Chem. Commun.* **2014**, *50*, 7103; b) P. Xiao, J. Gu, J. Chen, D. Han, J. Zhang, H. Cao, R. Xing, Y. Han, W. Wang, T. Chen, *Chem. Commun.* **2013**, *49*, 11167.
- [5] P.-G. de Gennes, *Angew. Chem. Int. Ed.* **1992**, *31*, 842.
- [6] F. Liang, C. Zhang, Z. Yang, *Adv. Mater.* **2014**, *26*, 6944.
- [7] a) Z. Zheng, C. T. Nottbohm, A. Turchanin, H. Muzik, A. Beyer, M. Heilemann, M. Sauer, A. Götzhäuser, *Angew. Chem. Int. Ed.* **2010**, *49*, 8493; b) L. Zhang, J. Yu, M. Yang, Q. Xie, H. Peng, Z. Liu, *Nat. Commun.* **2013**, *4*, 1443.
- [8] a) C. Zhang, W. W. Tjiu, T. X. Liu, *Polym. Chem.* **2013**, *4*, 5785; b) L. J. Cote, R. Cruz-Silva, J. Huang, *J. Am. Chem. Soc.* **2009**, *131*, 11027.
- [9] S. Iijima, T. Ichihashi, *Nature* **1993**, *364*, 737.
- [10] a) J. T. Di, D. M. Hu, H. Y. Chen, Z. Z. Yong, M. H. Chen, Z. H. Feng, Y. T. Zhu, Q. W. Li, *ACS Nano* **2012**, *6*, 5457;

- b) P. G. Collins, K. Bradley, M. Ishigami, A. Zettl, *Science* **2000**, 287, 1801; c) J. Kong, N. R. Franklin, C. W. Zhou, M. G. Chapline, S. Peng, K. J. Cho, H. J. Dai, *Science* **2000**, 287, 622; d) P. C. Collins, M. S. Arnold, P. Avouris, *Science* **2001**, 292, 706; e) E. T. Thostenson, Z. F. Ren, T. W. Chou, *Compos. Sci. Technol.* **2001**, 61, 1899; f) M. M. J. Treacy, T. W. Ebbesen, J. M. Gibson, *Nature* **1996**, 381, 678.
- [11] a) M. Yu, Y. Zhang, Y. Zeng, M.-S. Balogun, K. Mai, Z. Zhang, X. Lu, Y. Tong, *Adv. Mater.* **2014**, 26, 4724; b) Y. Zhao, J. Liu, Y. Hu, H. H. Cheng, C. G. Hu, C. C. Jiang, L. Jiang, A. Y. Cao, L. T. Qu, *Adv. Mater.* **2013**, 25, 591.
- [12] a) W. S. Li, P. X. Hou, C. Liu, D. M. Sun, J. T. Yuan, S. Y. Zhao, L. C. Yin, H. T. Cong, H. M. Cheng, *ACS Nano* **2013**, 7, 6831; b) M. C. LeMieux, S. Sok, M. E. Roberts, J. P. Opatkiewicz, D. Liu, S. N. Barman, N. Patil, S. Mitra, Z. Bao, *ACS Nano* **2009**, 3, 4089; c) J. Li, L. Niu, Z. Zheng, F. Yan, *Adv. Mater.* **2014**, 26, 5239; d) H. Wang, B. Cobb, A. van Breemen, G. Gelinck, Z. Bao, *Adv. Mater.* **2014**, 26, 4588; e) S. J. Choi, P. Bennett, K. Takei, C. Wang, C. C. Lo, A. Javey, J. Bokor, *ACS Nano* **2013**, 7, 798.
- [13] a) Q. Sun, D. H. Kim, S. S. Park, N. Y. Lee, Y. Zhang, J. H. Lee, K. Cho, J. H. Cho, *Adv. Mater.* **2014**, 26, 4735; b) Y. Wang, L. Wang, T. Yang, X. Li, X. Zang, M. Zhu, K. Wang, D. Wu, H. Zhu, *Adv. Funct. Mater.* **2014**, 24, 4666; c) N. Fukaya, D. Y. Kim, S. Kishimoto, S. Noda, Y. Ohno, *ACS Nano* **2014**, 8, 3285.
- [14] A. Lekawa-Raus, J. Patmore, L. Kurzepa, J. Bulmer, K. Koziol, *Adv. Funct. Mater.* **2014**, 24, 3661.
- [15] a) S. Zhang, K. K. K. Koziol, I. A. Kinloch, A. H. Windle, *Small* **2008**, 4, 1217; b) B. Vigolo, A. Penicaud, C. Coulon, C. Sauder, R. Pailler, C. Journet, P. Bernier, P. Poulin, *Science* **2000**, 290, 1331.
- [16] Y. L. Li, I. A. Kinloch, A. H. Windle, *Science* **2004**, 304, 276.
- [17] X. B. Zhang, K. L. Jiang, C. Teng, P. Liu, L. Zhang, J. Kong, T. H. Zhang, Q. Q. Li, S. S. Fan, *Adv. Mater.* **2006**, 18, 1505.
- [18] N. Behabtu, C. C. Young, D. E. Tsentelovich, O. Kleinerman, X. Wang, A. W. K. Ma, E. A. Bengio, R. F. ter Waarbeek, J. J. de Jong, R. E. Hoogerwerf, S. B. Fairchild, J. B. Ferguson, B. Maruyama, J. Kono, Y. Talmon, Y. Cohen, M. J. Otto, M. Pasquali, *Science* **2013**, 339, 182.
- [19] a) N. Rouhi, D. Jain, P. J. Burke, *ACS Nano* **2011**, 5, 8471; b) G. S. Tulevski, A. D. Franklin, D. Frank, J. M. Lobe, Q. Cao, H. Park, A. Afzali, S. J. Han, J. B. Hannon, W. Haensch, *ACS Nano* **2014**, 8, 8730.
- [20] X. Zhuang, Y. Mai, D. Wu, F. Zhang, X. Feng, *Adv. Mater.* **2015**, 27, 403.
- [21] a) F. Kim, L. J. Cote, J. Huang, *Adv. Mater.* **2010**, 22, 1954; b) J. Kim, L. J. Cote, F. Kim, W. Yuan, K. R. Shull, J. Huang, *J. Am. Chem. Soc.* **2010**, 132, 8180.
- [22] a) M. J. Allen, V. C. Tung, L. Gomez, Z. Xu, L.-M. Chen, K. S. Nelson, C. Zhou, R. B. Kaner, Y. Yang, *Adv. Mater.* **2009**, 21, 2098; b) T. R. Hendricks, J. Lu, L. T. Drzal, I. Lee, *Adv. Mater.* **2008**, 20, 2008; c) N. H. Kim, B. J. Kim, Y. Ko, J. H. Cho, S. T. Chang, *Adv. Mater.* **2013**, 25, 894.
- [23] a) H. Lu, Y. Yao, W. M. Huang, D. Hui, *Compos. Part B: Eng.* **2014**, 67, 290; b) H. Lu, F. Liang, J. Gou, *Soft Matter* **2011**, 7, 7416.
- [24] a) J. Gu, P. Xiao, J. Chen, F. Liu, Y. Huang, G. Li, J. Zhang, T. Chen, *J. Mater. Chem. A* **2014**, 2, 15268; b) J. Gu, P. Xiao, J. Chen, J. Zhang, Y. Huang, T. Chen, *ACS Appl. Mater. Interfaces* **2014**, 6, 16204.
- [25] Y. N. Xia, G. M. Whitesides, *Langmuir* **1997**, 13, 2059.
- [26] Y. Pan, H. Bao, L. Li, *ACS Appl. Mater. Interfaces* **2011**, 3, 4819.
- [27] M. Qian, Y. M. Pan, F. Y. Liu, M. Wang, H. L. Shen, D. W. He, B. G. Wang, Y. Shi, F. Miao, X. R. Wang, *Adv. Mater.* **2014**, 26, 3275.
- [28] S. Y. Yin, Y. Goldovsky, M. Herzberg, L. Liu, H. Sun, Y. Y. Zhang, F. B. Meng, X. B. Cao, D. D. Sun, H. Y. Chen, A. Kushmaro, X. D. Chen, *Adv. Funct. Mater.* **2013**, 23, 2972.